Macromolecular Chemistry and Physics
www.mcp-journal.de

Effect of Grafted Spiropyran on the Solubility and Film Properties of Photochromic Amylose

David Barsi, Elena Buratti, Antonio Tarantino, Franco Dinelli, Valter Castelvetro, and Monica Bertoldo**

Four photochromic spiropyran-amylose (ASP) biobased polymers with different spiropyran (SP) grafting density, DS, ASP_{10} (DS = 0.12), ASP_{40} and $ASP_{40}PA_{60}$ (DS = 0.40), and ASP_{100} (DS = 0.97), are synthesized through azide-alkyne cycloaddition of an alkynyl-functional SP derivative onto C6-azidated-amylose (AN_3), where the unconverted azide in $ASP_{40}PA_{60}$, ASP_{100}, and the AN_3 precursor are quenched by clicking with propargyl alcohol (PA). All ASPs are poorly soluble in trifluoroethanol, ethanol, and water but soluble in dimethyl sulfoxide, *N*,*N*-dimethylformamide, and hexafluoroisopropanol irrespective of UV irradiation, switching reversibly the grafted SP into zwitterionic merocyanine (MC). Only ASP_{10} and ASP_{40} are slightly soluble in the low polarity tetrahydrofuran, with ASP_{40} showing a marked photochromism and reduction of solubility on SP→MC switching. The photochromism in solution is preserved in the solid state, although with significant differences between the still relatively fast SP→MC photoisomerization and the much slower thermal retro-isomerization. The dynamics of both processes, evaluated in a thin spin–coated ASP_{100} film and a thicker ASP_{40} photoswitchable coating on glass and paper, is more clearly affected than in solution by the grafting density. Switching the nearly apolar SP into the zwitterionic MC does not significantly affect wettability of the slightly hydrophobic ASP_{40} coating.

1. Introduction

Photochromism, that is, the property of responding to photoexcitation by a reversible change in the optical properties of a material and, in particular, by a change in its absorption spectrum in the visible region, has been intensively investigated for its potential applications, among others, to produce stimuli-responsive materials. Applications of photochromic materials have been envisaged and, to different extents, investigated for different fields such as medicine,[1–7] biotechnology,[8–11] actuators,[12] optical data storage,[13–15] security documents,[16–18] chemical sensors,[11,19–27] and ophthalmic lenses.[28] The response of a photochromic material can be tuned, in principle, by appropriate selection of the photochromic moiety. However, the overall effectiveness in terms of sensitivity to the incident light, selectivity to specific wavelengths, reversibility under dark conditions, kinetics of the direct (under light irradiation) and reverse (upon light switch off) processes, and stability of the interchanging species under different conditions (pH, ionic strength, temperature, etc.) can be strongly affected by the matrix environment. In particular, the interaction with solvating or coordinating low molecular weight species may provide additional features to the photochromic material (e.g., solvatochromic responsiveness), while attachment of the photochromic dye to a solid surface or to a polymer may affect the kinetics, induce, or inhibit altogether, photo- and thermally-activated processes.

A potentially interesting class of photochromic materials consists of natural polymers modified by attachment of

D. Barsi, A. Tarantino
Institute for Chemical-Physical Processes of the National Research Council
CNR-IPCF, Area della Ricerca
via G. Moruzzi 1, Pisa I-56124, Italy

The ORCID identification number(s) for the author(s) of this article can be found under https://doi.org/10.1002/macp.202300092

To the memory of the longtime friend and colleague Mauro Aglietto

DOI: 10.1002/macp.202300092

E. Buratti, M. Bertoldo
Department of Chemical, Pharmaceutical and Agricultural Sciences
University of Ferrara
via L. Borsari, 46, Ferrara I-44121, Italy
E-mail: monica.bertoldo@unife.it

F. Dinelli
National Institute of Optics of the National Research Council
CNR-INO, Area della Ricerca
via G. Moruzzi 1, Pisa I-56124, Italy

V. Castelvetro
Department of Chemistry and Industrial Chemistry
University of Pisa
via G. Moruzzi, 13, Pisa I-56124, Italy

E-mail: valter.castelvetro@unipi.it

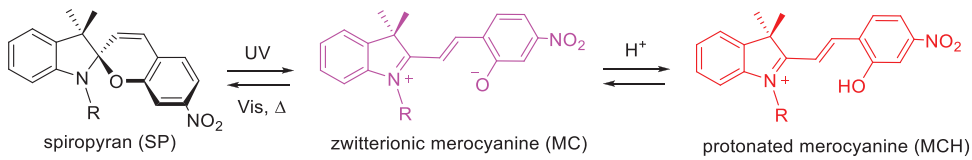

Scheme 1. Spiropyran (black), zwitterionic merocyanine (violet), and protonated merocyanine (red).

photochromic dyes.[3] Natural polymers are renewable, largely available, and generally considered as low environmental impact materials because of their sourcing from non-fossil biomass and their usual biodegradability at the end of their lifecycle. Besides, the high density of functional groups evenly distributed along the backbone possessing a more or less differentiated reactivity (e.g., primary and secondary alcohol as well as amine groups in polysaccharides such as cellulose, amylose, and chitosan) may be exploited for multiple functionalization processes.[29] Owing to these peculiar properties, the resulting biobased photochromic polymers may be employed for applications in which adhesion and enhanced compatibility with either biological tissues or biopolymers (e.g., cellulose, and collagen fibers and films), biodegradability, and low cost are desired features and may allow the production of disposable smart responsive materials and devices.

Among the various photochromic materials, spiropyran (SP) derivatives are particularly attractive because of the multiple effects resulting from the photo-induced isomerization. Typically, SP molecules absorb in the UV region to yield the corresponding colored and fluorescent merocyanine (MC) (**Scheme 1**); such conversion results in major changes not only in the optical properties,[13,30] but also in physical properties since the MC form has a different (more coplanar) conformation and is stabilized in its zwitterionic form, being thus characterized by a high dipolar moment.[20,31,32] As a consequence, the interchange between the SP and MC forms results in significant effects on the hydrophilic/hydrophobic character.[33,34]

Several strategies have been reported so far for the synthesis of polymeric structures bearing spiropyran moieties in the side chain. Among them, the Huisgen's 1,3-dipolar azide-alkyne cycloaddition, one of the so called "click" reactions,[29] has emerged for its effectiveness in grafting SP derivatives onto synthetic (polyacrylates and polycarbonates), bio-based (poly-α-hydroxy acids), and natural polymers (DNA, cellulose, and chitosan).[1,3–6,20,35,36] In the case of amylose, the linear polysaccharide in starch, the Huisgen's reaction has been used for grafting a wide range of molecular or even macromolecular side chains.[8–11,13–16,37,38] Among them, the preparation of spiropyran-functional amylose derivatives (ASP) by selective C6-azidation of the repeating glucopyranoside units, followed by Cu(I) catalyzed azide-alkyne cycloaddition of alkynyl spiropyran moieties, was reported by our group.[37]

While our previous paper aimed at describing the synthesis and the molecular characterization of the prepared ASPs, the main goal of the present research was to investigate the potential of such ASPs, featuring different degree of substitution (DS) with SP, as photoswitchable coating materials. For this purpose a preliminary study was carried out to assess the solubility of the ASPs in solvents of different polarity, to identify the most stable isomer form among SP, MC, and protonated merocyanine (MCH) under normal (temperature, light exposure) conditions, and to evaluate the photoresponse upon UV irradiation as well as the retro-isomerization kinetics as a function of solvent and DS.

The persistence of photochromism and its thermal reversibility also in the solid state cannot be taken for granted for a polymeric material characterized by a relatively rigid backbone such as amylose. For this purpose both thin films prepared by spin coating and thicker/less uniform films prepared by casting on glass or dip coating on paper were evaluated. The filmability, photoresponse, and reversibility in the dark of the SP→MC or MC→SP isomerization in the solid state were finally evaluated. Such photochromic ASP polymers were expected to be particularly suitable as coatings for paper, given the affinity between cellulose and the amylose polymer backbone.

2. Experimental Section

2.1. Materials and Reagents

Amylose from potatoes (type III) was purchased from Aldrich and dried at 50 °C and 0.5 mmHg overnight before use. Its number average molecular weight was 47.7 ± 6.2 kDa by colorimetric titration of the terminal aldehyde[2] and 19.8 kDa by SEC analysis in 0.5 M aqueous NaCl with polyethylenoxide as standard for the calibration. The synthesis of 3′,3′-dimethyl-6-nitro-1′-(prop-2-yn-1-yl)spiro[chromene-2,2′-indoline] (SPCC) and of amylose azidated by regioselective and exhaustive substitution of the hydroxyl groups at the C6 position of the glucopyranoside repeat units (AN_3) had been previously described.[37] Dimethylformamide (DMF) was distilled over $MgSO_4$ (53 °C, 18 mmHg). Dimethylsulfoxide (DMSO) was distilled over CaH_2 (82 °C, 18 mmHg). Tetrahydrofuran (THF) was dried over $CaCl_2$, refluxed over metallic Na and benzophenone (0.2% w/v), distilled and stored over 4A molecular sieves in the dark in a N_2 atmosphere. Amylose from potatoes was purchased from Sigma-Aldrich. Copper(I) chloride (97%), propargyl alcohol (PA) (Sigma-Aldrich, 99%) trifluoroethanol (TFE), and hexafluoroisopropanol (HFIP) (Sigma-Aldrich) were used as received.

2.2. Photochromic Amyloses

Five amylose derivatives, differing in the degree of substitution (DS = moles of grafted SP/moles of glucopyranose units) with photochromic SP moiety attached to the glucopyranoside C6 position through a triazole bridging linkage, were prepared. The polysaccharide functionalization was accomplished by Cu(I) catalyzed azide-alkyne cycloaddition of the alkynyl derivative SPCC onto AN_3 as previously described (**Scheme 2**).[37] In particular, amylose was azidated by following the procedure described by J. Shey et al.[39]. Yield, calculated as the mass ratio between the recovered modified polysaccharide and theoretical fully azidated

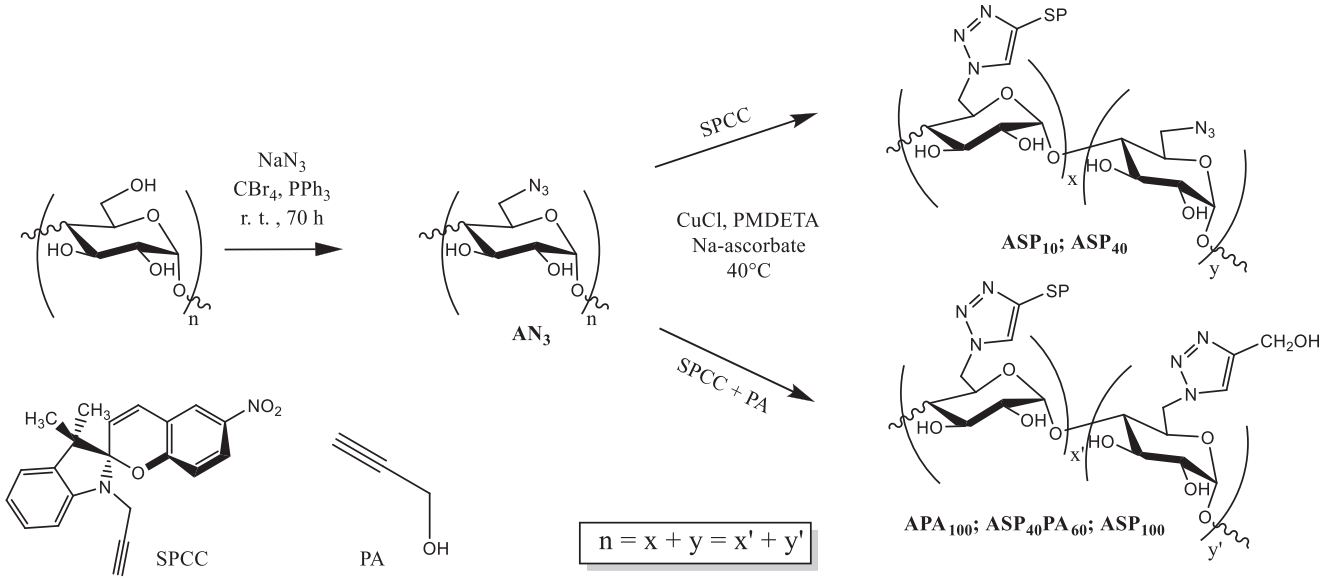

Scheme 2. Structures and synthesis of spiropyran-functionalized amyloses.[37]

product (AN_3), was of 82%. The presence of azide groups in AN_3 was assessed by IR and ^{13}C-NMR spectroscopy analyses showing the azide stretching at 2096 cm^{-1} and the azidated C6 resonance at 51 ppm, respectively. In the second reaction step, C6-azide groups in the AN_3 intermediate were partially (samples ASP_{10} and ASP_{40}) or totally reacted with propargyl groups (samples $ASP_{40}PA_{60}$ and ASP_{100}) (Scheme 2). Derivatives with different amounts of grafted SP groups were obtained by adjusting the SPCC/azide feed ratio. Propargyl alcohol was fed together with SPCC at a slight total SP+PA molar excess with respect to the glucosidic units to ensure full conversion of the azide groups in the case of samples $ASP_{40}PA_{60}$ and ASP_{100} (DS = 0.97).

In short, a slight stoichiometric excess of the required SPCC, PA or SPCC/PA mixture was added to a DMSO solution of AN_3 (0.2 mol L^{-1} azide groups), then the catalyst (CuCl/PMDETA 1/1 mole ratio in DMSO) was added under nitrogen, followed by 4 M sodium ascorbate aqueous solution (0.25 equiv.). After stirring at 40 °C for a few days up to the consumption of the reactants (SPCC checked by TLC and the residual azide groups by FT-IR spectroscopy) the product was purified by twofold precipitation from DMSO/ethanol, redispersion in distilled water, dialysis (MWCO 1 kDa) first against a 2 mol·L^{-1} aqueous EDTA then against pure water, followed by lyophilization. Yield, as weight of recovered modified polysaccharide over the azidated polysaccharide plus the total alkynes in the reaction feed, was 80–85%.[37]

The following SP-functionalized amylose derivatives were obtained: ASP_{10} (DS = 0.12), ASP_{40}, and $ASP_{40}PA_{60}$ (DS = 0.40), and ASP_{100} (DS = 0.97); in addition, the precursor AN_3 (DS = 0) and APA_{100}, a derivative obtained by exhaustive reaction of the azide moieties with propargyl alcohol, were also used as reference materials bearing no grafted SP moieties.

ATR FT-IR spectra (cm^{-1}): AN_3, 3325 (ν, O–H), 2919, 2513, (ν, CH_2 and CH), 2098 and 2036 (ν, N=N), 1438 (ν, C–N), 1282, 1150 and 1078 (ν, C–O glucosidic ring), 999, 849, 758, 559. ASP_{10}, 3351 (ν, O–H), 2923 (ν, CH_2), 2102 (ν, N=N), 1607 (ν, C=C), 1580 (ν, N–O), 1483 (δ, C–H aliphatic), 1458 (δ, CH_2), 1439, 1335 (δ, CH_2), 1279, 1151, and 1077 (ν, C–O glucosidic ring), 1040, 1011, 949, 919, and 748 (δ, C–H aromatic). ASP_{40}, 3369 (ν, O–H), 2919 (ν, CH_2), 2112 (ν, N=N), 1608 (ν, C=C), 1579 (ν, N–O), 1481 (δ, C–H aliphatic), 1459 (δ, CH_2), 1437, 1335 (δ, CH_2), 1272, 1151, and 1087 (ν, C–O glucosidic ring), 1032, 1014, 949, 911, 835, 808, 747 (δ, C–H aromatic). $ASP_{40}PA_{60}$, 3390 (ν, O–H), 2922 (ν, CH_3); 1612 (ν, C=C), 1516 (ν, N–O), 1483 (δ, C–H aliphatic), 1459 (δ, CH_2), 1405; 1338 (δ, CH_2), 1271, 1227, 1153, and 1079 (ν, C–O glucosidic ring), 1041, 950, 920, 751 (δ, C–H aromatic). ASP_{100}, 3423 (ν, O–H), 2927 (ν, CH_3), 1608 (ν, C=C), 1516 (ν, N–O), 1483 (δ, C–H aliphatic), 1459 (δ, CH_2), 1338 (δ, CH_2), 1266, 1155, and 1090 (ν, C–O glucosidic ring), 1035, 949, 915, 810, and 748 (δ, aromatic C–H). APA_{100}, 3435 (ν, O–H), 2926 (ν, CH_3), 1634 (ν, C=C), 1409, 1232, 1155, 1143, 791, and 763.

The ^{1}H NMR spectra in DMSO-d_6/D_2O 75/25 of clicked products showed broad signals in the 3.0–5.2 ppm range due to amylose, at 6.5 and 8.2 ppm (Ar–H), 5.8 and 6.0 ppm, (C=C–H of SPCC), 0.7–1.5 ppm range (CH_3) of SPCC, and at 7.7 ppm the proton of the triazole ring superimposed to other SPCC signals. The average number of grafted SP per glucopyranose unit, DS, was calculated from the ratio between the peak integral of the spiropyran unresolved methyl resonances and that of the anomeric proton of amylose at 5.15 ppm.[37] Possible change in the average molecular weight of amylose after modification was checked for APA_{100}, the only derivative whose ^{1}H NMR spectrum had well resolved peaks. The intensity ratio between the ^{1}H signals at 4.9 and 5.15 ppm attributed to the H4 proton of the non-reducing glucopyranose chain-end[40] and to the H1 proton of the internal glucopyranose units, was comparable to the one observed in the pristine amylose, thus indicating that no significant change in the backbone length occurred throughout the chemical modification steps. Since the reaction conditions were the same for all derivatives, it is reasonable to assume that the backbone length for all amylose derivatives was similarly unaffected and comparable with that of the pristine natural polymer.

2.3. Instruments and Methods

UV–Vis absorption spectra were recorded in the 300–700 nm range using either a Perkin-Elmer Lambda 25 spectrophotometer for solutions in 1 cm quartz cells, or an Agilent Cary 5000 UV–vis–NIR instrument for cast films on glass. Pure solvent and pristine glass were used as reference for the analysis of the polysaccharide solutions and coating films, respectively. Spectra registered with pure solvents or glass as samples were used for baseline correction. The Microcal Origin software (OriginLab Corp., Northampton, MA, USA) was used for spectral correction and analysis.

AN_3 and ASP films were prepared by casting or dip coating using polymer solutions in DMF (5 mg mL^{-1}). Glass slides was cleaned by rinsing with acetone, 2-propanol, and DMF, followed by drying in an oven at 150 °C for 3 h, were used to prepare cast films by spreading a uniform layer of the given polymer solution that was then allowed to dry in the dark at room temperature in a fume hood for 5 days. Dip-coated paper samples were prepared by soaking filter paper disks (3 cm diameter, Whatman grade 1) in the polymer solution for 2 min, then the disk was slowly withdrawn to allow draining of the excess solution before placing it on a glass slab, followed by drying in the dark at room temperature in a fume hood for 5 days.

Films by spin coating were obtained on glass coverslips using HFIP solutions (5 mg mL^{-1}). A drop (80 µL) of the solution was spread all over the 10 × 10 mm glass surface, then spinning was started at 500 rpm s^{-1} and carried out at 1000 rpm for 90 s. The glass surface was previously washed twice with 2-propanol, then dried under a N_2 flux, sonicated in aqueous 10% NaOH for 5 min and finally rinsed twice in water. The procedure was repeated twice, then the obtained activated glass was stored in water at 4°C and dried under N_2 purge just before use.

The surface morphology of the films was recorded with an AFM consisting of a commercial head (mod. SMENA, NT-MDT Spectrum Instruments, Ireland) equipped with electronics and in-house developed control software. The AFM was operated in the so-called tapping mode, employing cantilevers with a nominal spring constant of around 5–15 N m^{-1} and a resonant frequency of a few hundred kHz (NT-MDT, NSG11). The color code of the images was the following: a brighter color corresponds to a higher region.

Irradiation with UV-A light was accomplished during 10 min, unless otherwise specified, by means of a 25 W fluorescent Wood lamp (GBC spiral light T3 Black, from Kon.El.Co. SpA, Italy) placed at 10 cm from the sample.

ASP solutions were prepared by addition to the given solvent (water, DMF, DMSO, THF, TFE, HFIP, and ethanol) of the required amount of a concentrated ASP solution in DMSO (10 mg mL^{-1}) obtained by stirring for 24 h at 70 °C.

Static water contact angle measurements were performed on a KSV CAM 200 goniometric apparatus. The reported contact angle values were the average of at least six measurements performed by depositing with a microsyringe, a 13 µL droplet of deionized water in different spots of the sample surface, and recording the contact angle as quickly as possible to avoid artefacts due to the modification of the film surface as a result of water vapor adsorption.

Table 1. Solvatochromic Dimroth–Reichardt polarity indices E_N^T of the solvents tested for ASP_{40}[41].

Solvent	HFIP	Water	TFE	Ethanol	DMSO	DMF	THF
E_N^T	1.068	1	0.898	0.654	0.444	0.386	0.207

3. Results and Discussion

3.1. Solubility of the SP-Amylose Polymers in Solvents of Different Polarity

In order to evaluate the combined effects of the solvent type, of the degree of substitution (DS), and of the photoisomerization on the solubility of the spyropiran-grafted amylose (ASP), systematic solubility tests were performed on ASP_{40}, that is, the polysaccharide with an intermediate DS. Six solvents were selected, according to their different H-bonding character and polarity decreasing in the order: 1,1,1,3,3,3-hexafluoro-2-propanol (HFIP), water, trifluoroethanol (TFE), ethanol, dimethyl sulfoxide (DMSO), *N*,*N*-dimethylformamide (DMF), and tetrahydrofuran (THF).[41] In **Table 1** are reported the corresponding values of the normalized solvatochromic Dimroth–Reichardt polarity index, E_N^T. The latter is a dimensionless empirical parameter obtained from the transition energy of the longest wavelength charge transfer absorption band of the betaine dye 2,6-diphenyl-4-(2,4,6-triphenyl-1-pyridino)-phenoxide in dilute solution in the given solvent, normalized according to a scale assigning the values of $E_N^T = 1.00$ to water and $E_N^T = 0.00$ to the apolar tetramethylsilane (TMS, Equation (1)).

$$E_T^N = \frac{E_T(\text{solvent}) - E_T(\text{TMS})}{E_T(\text{water}) - E_T(\text{TMS})} = \frac{E_T(\text{solvent}) - 30.7}{32.4} \quad (1)$$

The betaine phenoxide dye exhibits a very high sensitivity to solvent polarity, with hypsochromic shifts covering a large wavelength range for solvents of increasing polarity.

Upon stirring in the given solvent at 1 mg mL^{-1} for 36 h in the dark, ASP_{40} gave limpid yellowish solutions in DMF and DMSO, and a red solution in HFIP. The good solubility in the three solvents is proved by the negligible light scattering (apparent absorption) at 750 nm (**Figure 1**, left), a spectra region where no absorption occurs. Well detectable light scattering at 750 nm was instead observed for the sample in water, TFE, and ethanol, all solvents with quite high E_N^T values (Table 1). In these solvents, only moderately stable dispersions could be formed, resulting in the slow formation of a precipitate. Similarly, pristine amylose is insoluble in water but it does solubilize in DMSO, DMF, and HFIP, an indication that the solubility of the obtained amylose derivatives is scarcely affected by the grafted groups and it mainly depends on the backbone behavior.

Upon irradiation, further reduction of solubility was observed in TFE and THF, the larger relative changes in solubility being observed for THF, although TFE was still comparably less effective as a solvent even after irradiation (Figure 1, right). This reduction can be ascribed to the increased polarity of the functional polymer as a result of the photoisomerization of the grafted spiropyran moieties into the zwitterionic merocyanine isomeric

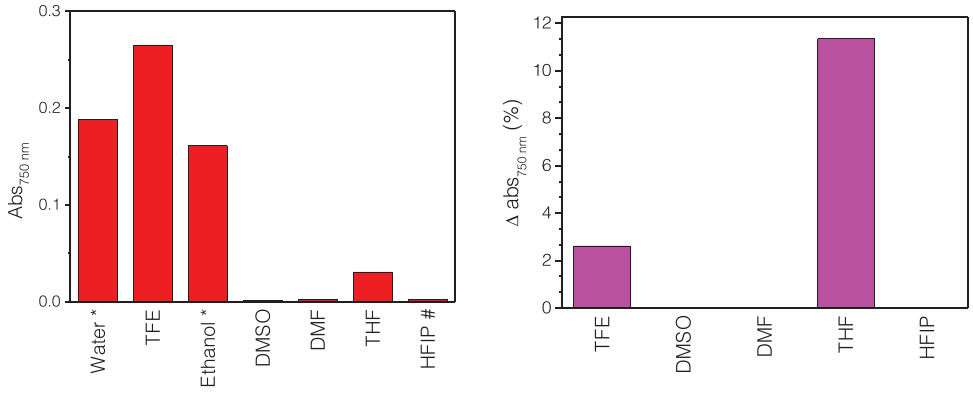

Figure 1. Apparent absorbance at 750 nm due to light scattering of particulate matter in freshly prepared 0.1 mg mL^{-1} solutions/suspensions of ASP_{40} (left) in the given solvent, and variations recorded after UV–vis irradiation (right). *Data are only indicative because sedimentation occurred during the acquisition time. #ASP_{100} was used in the case of HFIP.

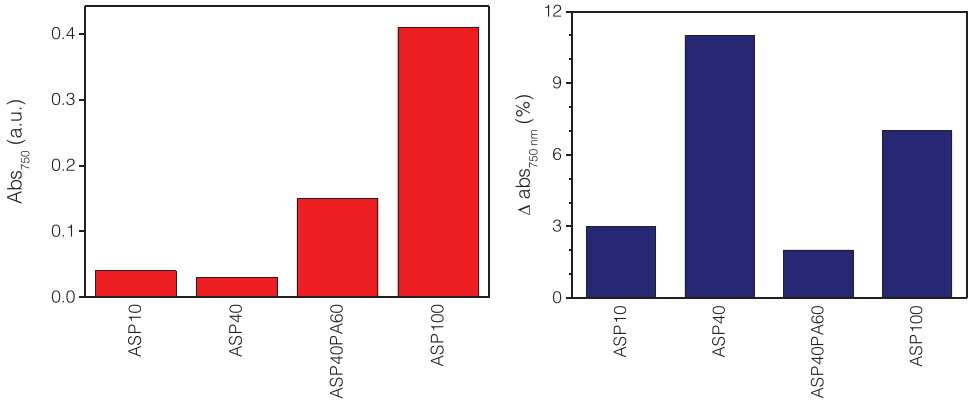

Figure 2. Apparent absorbance at 750 nm before irradiation (left) and absorbance percent variation ΔAbs_{750nm} after UV irradiation (right) of ASP_{40} in THF.

form. Thus the grafted groups as well as the SP/MC form do affect to some extent the solubility of the polysaccharide. Being a reasonably effective but borderline solvent for ASP_{40}, THF was then selected as a test solvent to evaluate the solubility of each one of the different ASP derivatives, all of which turned out to be less soluble than ASP_{40} both before and after irradiation (**Figure 2**). Based on the optical density due to scattering at 750 nm the less soluble among the modified polymers was ASP_{100}, while ASP_{10} appeared as the most soluble. This is counterintuitive, as the solubility in the low polarity THF was expected to be higher for ASP_{100} that bears the largest amount of apolar SP moieties. One can thus speculate that a combination of effects contributes to the observed behavior. In fact, the low solubility of amylose in water has been ascribed to the formation of ordered structures mainly stabilized by inter-chain hydrogen bonds.[42,43] Amylose is soluble only in the presence of chemical species able to interrupt these hydrogen bridges. In our case, grafting the SP moieties at the less sterically hindered and most conformationally mobile C6 in the glucosidic units seems to scarcely affect the ability of amylose to self-assemble into the densely packed helical structures typical of its crystalline forms. On the other hand, replacement of each OH group of amylose with an azide that, unlike the –OH groups in the pristine amylose or in APA_{100}, cannot form inter- or intra-chain hydrogen bonds, results in lower strength of the amylose inter-chain interaction and thus enhanced solubility. Inter-chain H-bonding is again possible and solubility lowered when the grafted azide is reacted with PA bearing an alcoholic group. This is shown by the solubility of AN_3 in THF that was observed to decrease upon complete replacement of the azide with propargyl groups in APA_{100}, the latter being insoluble and not dispersible in THF. Overall, the good solubility of ASP_{40} is likely the result of a good match between the polarity of the solvent and that of the SP-functional polymer. The slightly better solubility of ASP_{40} than that of $ASP_{40}PA_{60}$ may be ascribed to the higher density of H-bonding hydroxy groups in the latter, and thus a possibly higher density of inter-chain hydrogen bonding.

Upon irradiation, variations of optical density at 750 nm due to scattering by suspended ASP particulate were detected for all investigated samples, APA_{100} included (Figure 2). Since the latter has no bonded photochromic moieties, the variation is unlikely to be simply related to a specific photoactivated process; indeed, a random and apparently not negligible contribution to the measured optical density values comes from the intrinsic variability of the optical density measurements that were performed before and after irradiation. However, when comparing the samples with similar good solubility (as deduced from the low and comparable optical density at 750 nm) ASP_{10} and ASP_{40}, the significantly larger variation on irradiation observed for the latter is

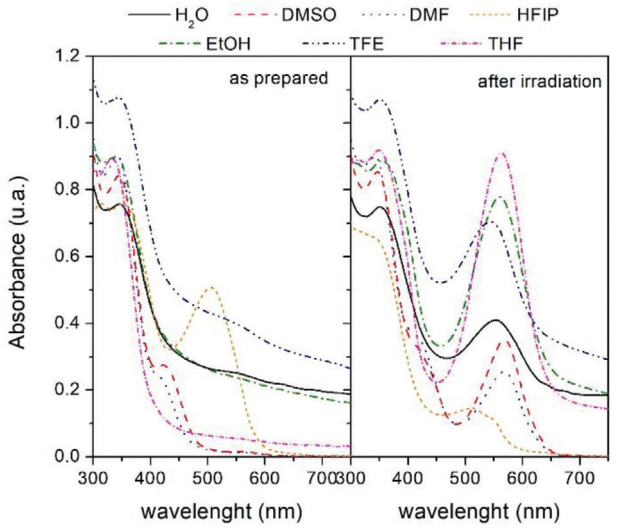

Figure 3. UV–vis spectra of ASP_{40} in different solvents (0.1 mg mL^{-1}) before (left) and after (right) irradiation with UV light.

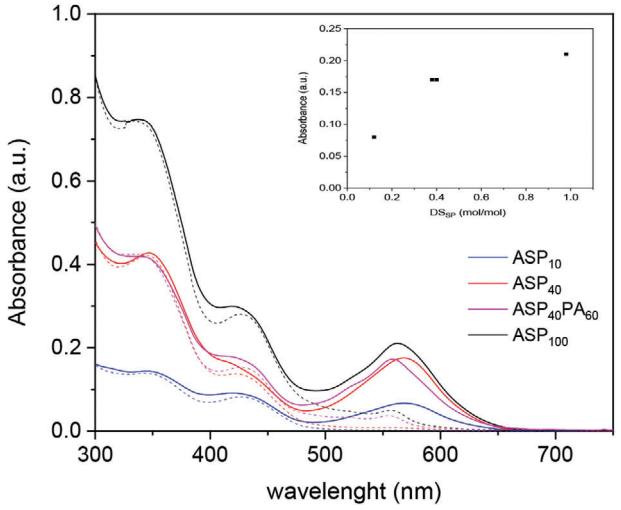

Figure 4. UV–vis spectra in DMSO (0.05 mg mL^{-1}) before (dash lines) and after (solid lines) irradiation with UV light and maximum band intensity of the MC absorption band after UV irradiation as a function of DS (inset).

indicative of an active role of the grafted SP on the variation of the solubility of ASP.

No settling was detected in HFIP, DMF, and DMSO, which were found to be good solvents of the ASP derivatives irrespective of DS and of the actual SP/MC ratio (Figure 1). In particular, while the large E_N^T values of DMSO and DMF (Table 1) indicate their good solvency for the polymers even after photoisomerization of SP into the zwitterionic MC, HFIP has such a high a E_N^T value that the MC form becomes actually the most stable form even under dark conditions.

3.2. Photoisomerization of ASP40 in Solvents of Different Polarity

ASP_{40} was selected among the synthesized SP-amylose polymers to study the photoisomerization process in detail, because it displayed the best combination of a good solubility when the residues are in the spiropyran form, and the largest change in solubility upon switching them into the MC form.

In **Figure 3** the UV–vis spectra in the 300–750 nm range, recorded from diluted (0.1 mg mL^{-1}) ASP_{40} solutions/dispersions, show the typical main absorption from the cyclic spiropyran with λ_{max} = 340–345 nm in all solvents but THF, in which λ_{max} is shifted at 332 nm. A shoulder at $\lambda \approx$ 400–440 nm that can be ascribed to the MCH form is also present in the aprotic DMF and DMSO.[44] The red transparent HFIP solution presents an intense absorption by the open zwitterionic merocyanine (MC) with λ_{max} = 508 nm. A weak and broad absorption with $\lambda_{max} \approx$560 nm, indicative of the presence of a small fraction of SP groups isomerized in the MC form, can also be detected in the spectra of ASP_{40} in all the other solvents. This adsorption is superimposed to a background scatter throughout the visible region in the case of the poorest solvent (water, ethanol, TFE, and, to a lesser extent, THF).

All the ASP_{40} solutions/dispersions obtained after 36 h of stirring exhibited color change once irradiated with UV or green light due to the photochromism of the spiropyran moieties bound to amylose. The UV–vis spectra of the irradiated solutions/dispersions showed an increased intensity of the merocyanine π–π^* absorption band with λ_{max} in the 545–565 nm range in all solvent except HFIP, in agreement with the observed color changes. The absorption band of the protonated merocyanine form (MCH) was only slightly affected by irradiation, causing no appreciable wavelength shift and a modest increase of absorbance most likely due to the superposition with the MC one.

The hue developed after irradiation and the rate of subsequent bleaching in the dark depended on the solvent, as typically observed for the unbound SP chromophore.[1,29] In particular, the ASP_{40} solutions in DMF and DMSO, as well as the dispersion of solvent-swollen particles in THF, turned quickly violet on UV irradiation and bleached out in less than 30 min in the dark. On the other hand, the retro-isomerization of the ASP_{40} particle dispersions in ethanol required several hours, while it did not proceed at all in water within 3 days in the dark, indicating a high stability (or long relaxation time) of the violet merocyanine form of the chromophore in the solid (particle) state, as previously reported for similar systems.[2,3] Interestingly, inverse photochromism was observed in HFIP: its red ASP_{40} solution being unaffected by UV irradiation but bleaching to a pale orange-yellow upon green light irradiation, in agreement with a previously reported behavior of a SP-grafted polypeptide in this solvent.[4]

3.3. Effect of the Grafting Density on the Photoisomerization and Retro-Isomerization Kinetics in Solution

The effect of the grafting density DS on the SP→MC photoisomerization have been previously studied for the same SP-functional amyloses in DMF, in which the functionalized amyloses are soluble irrespective of DS,[37] and the intensity of the MC absorption band appearing upon irradiation with UV light increases linearly with increasing DS. A slightly different result was instead obtained here when studying the solutions in DMSO, where the MC band intensity was observed to increase less than linearly at increasing DS (**Figure 4**), with a slight hypsochromic shift as a result of further substitution of the azides with PA. The hypsochromic effect on the MC absorption, typically ascribed

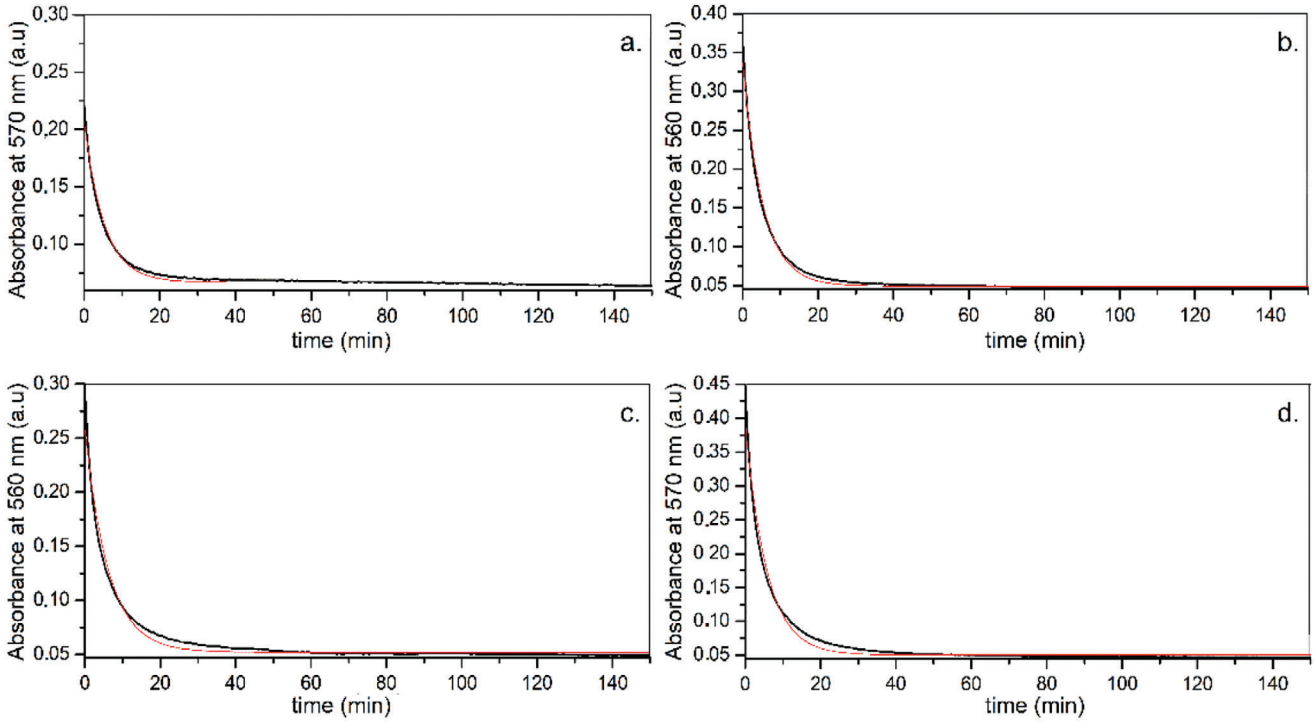

Figure 5. MC→SP retro-isomerization kinetics of a,c) $ASP_{40}PA_{60}$ and b,d) ASP_{100} in a,b) DMSO and c,d) DMF solutions (0.1 mg mL^{-1}): experimental curve (black) and exponential fitting (red).

to a lower polarity environment, is larger in $ASP_{40}PA_{60}$ than in ASP_{100} (with nominal DS = 100 but actually carrying a few PA residues), suggesting a prevailing role of the less polar triazole ring over the polarity of the hydroxymethylene group in the triazole derivative generated by the PA grafting.

The retro-isomerization kinetics in DMF and DMSO solutions was studied for $ASP_{40}PA_{60}$ and ASP_{100} by following the MC band intensity over time in the dark (**Figure 5**). The experimental data were interpolated with the exponential function (1), to obtain the retro-isomerization half-life τ parameters (1).

$$A_{\lambda max} = \alpha\, e^{-\frac{x}{\tau}} + A_{\infty} \quad (2)$$

The good fit (coefficient of correlation $R^2 > 0.98$) obtained with the first order exponential equation for all four sets of experimental data (see Figure 5) indicates that the retro-isomerization kinetic mechanism is satisfactorily described as a monomolecular process in both solvents and for both DS values. The obtained kinetic parameters indicate a slightly faster process (smaller τ values) in DMSO than in DMF. Furthermore, while the retro-isomerization in DMF is slower for $ASP_{40}PA_{60}$ than for ASP_{100}, the substitution degree has a negligible effect on the same process in DMSO (**Table 2**).

Table 2. Kinetic parameters of the MC→SP retro-isomerization for $ASP_{40}PA_{60}$ and ASP_{100} in DMF and DMSO.

Sample	Solvent	τ (min)	R^2
$ASP_{40}PA_{60}$	DMSO	5,24 ± 0,02	0986
ASP_{100}	DMSO	5,29 ± 0,02	0994
$ASP_{40}PA_{60}$	DMF	6,23 ± 0,03	0982
ASP_{100}	DMF	5,69 ± 0,03	0984

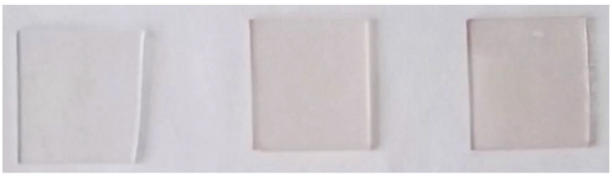

Figure 6. APA_{100} (left), $ASP_{40}PA_{60}$ (center), and ASP_{100} (right) spin coated films on activated glass.

3.4. Effect of the Grafting Density on Film Formation

In order to study the effect of DS on the film formation, 100–300 nm-thick films were prepared by spin coating solutions in HFIP of $ASP_{40}PA_{60}$ and ASP_{100} on thin glass coverslips. APA_{100} was also studied as reference. Among the solvents able to solubilize the polymer (Figure 1), HFIP was selected, being much more volatile than DMSO and DMF and thus easier to remove from the spin coated film. Uniform spin coated films could be obtained with $ASP_{40}PA_{60}$, ASP_{100} and APA_{100} covering the whole range of DS values. Both ASP films exhibited a pale pink color of increasing intensity with increasing DS, as already observed for the respective solutions (**Figure 6**).

Since in the case of thin films the surface of the substrate may affect the properties of the film during and after its deposition,

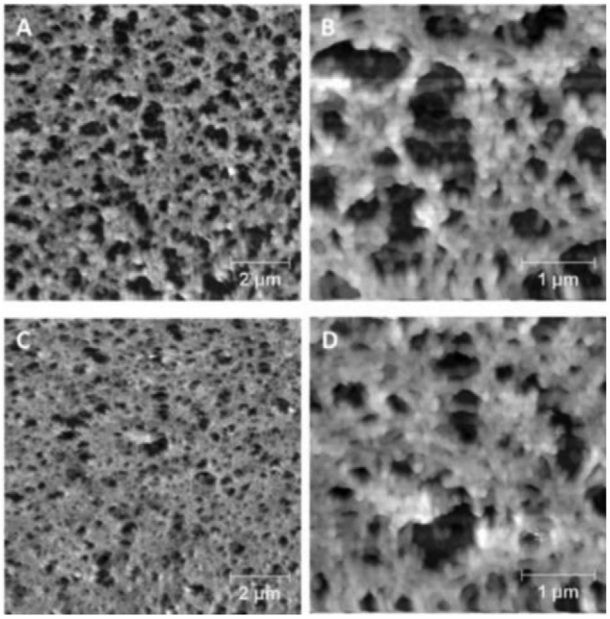

Figure 7. A–D) AFM topography images of ASP_{100} films on glass (A and, at higher magnification, B) and on activated glass (C and, at higher magnification, D).

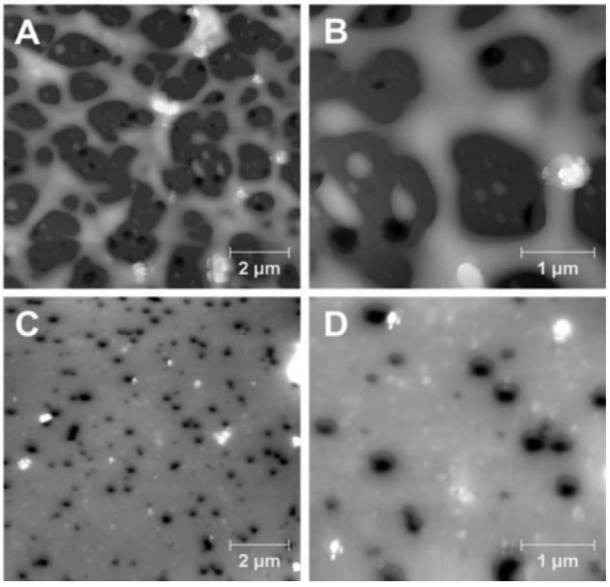

Figure 8. A–D) AFM topography images of $ASP_{40}PA_{60}$ (A and, at higher magnification, B) and APA_{100} films on activated glass (C and, at higher magnification, D).

the polymers were spin coated on both pristine and activated glass and then analyzed by atomic force microscope (AFM), to highlight any differences that may be associated with the substrate pre-treatment.

Activated glass surface was obtained by treatment with hot NaOH in an ultrasound bath. The high silanol concentration generated on the glass surface by the alkaline treatment results in higher affinity and improved wettability with a polar solvent such as HFIP, enhanced hydrogen bond interactions with the polysaccharides, and thus better adhesion of the (modified) polysaccharides on the glass.

ASP_{100} films showed a morphology apparently consisting of partially coalesced spheroidal particles about 100 nm in size, and a high porosity with pores larger on untreated glass (≈400 nm) (**Figure 7**A,B) than on activated glass (≈200 nm) (Figure 7C,D). The particle-like morphology could be ascribed to incipient nanoprecipitation of the poorly soluble polymer during fast solvent evaporation, and the apparently denser film morphology on activated glass to a better interfacial interaction between solvent and glass surface possibly resulting in slower evaporation.

The AFM images of spin coated $ASP_{40}PA_{60}$ and APA_{100} on activated glass showed completely different film surface morphologies, without the particle-like structures previously observed in ASP_{100} and smoother although still nanoporous surfaces, indicating a better polymer–solvent affinity along with some plasticizing effect of the residual solvent during the final stage of evaporation (**Figure 8**A,B). In particular, pores were about 200 nm in size for $ASP_{40}PA_{60}$ and smaller with an overall much denser film for APA_{100} (Figure 8C,D). Such better filmability is clearly correlated with the different solubility in HFIP of the polymers depending on the SP and PA content, with APA_{100} giving the smoothest and more homogeneous film, and ASP_{100} the most porous and irregular at the nanoscale.

3.5. Photoisomerization in the Solid State

The UV–vis spectroscopic characterization of the optical properties and photoisomerization in the solid state were studied on ASP_{100}, as it could be prepared as a relatively smooth thin film by spin coating from HFIP solution while providing the highest SP absorption, and possibly the largest effects due to SP crowding in the solid state as compared to the corresponding solution. The absorption spectrum of the as prepared ASP_{100} film showed the same two maxima at 560 and ≈400 nm (**Figure 9**a) as those in the HFIP solution (see Figure 3), indicating the presence of at least a fraction of grafted SP in the MC form. Irradiation of the film with UV or green light resulted in only minor spectral changes. On the other hand, when the film was kept in the dark the originally pink color bleached, although at a very slow rate, with the MC adsorption band intensity decreasing to half its initial value after about 3 weeks (Figure 9a). When the film was observed again after 1 year in the dark, it was completely colorless, in agreement with the disappearance of the MC band at 560 nm. However, the optical properties of the freshly spin coated film could be regained by irradiating the film with UV light for just a few minutes, as confirmed by the UV–vis spectra in Figure 9b showing the parallel decrease of the SP band below 400 nm and increase of the MC adsorption at 560 nm.

Covalent SP attachment to a macromolecular chain has been reported to slow down the retro-isomerization process[45] by limiting the conformational mobility involved in the cleavage/formation of the C–O-pyran bond. The latter occurs with associated rotation of one portion of the molecule around its long axis so as to approach coplanarity, a phenomenon emphasized in the solid state as compared to the polymer in solution.[46] Such conformational change is further hindered if the amorphous phase of the polymer is in a glassy state, as in the case of unplasticized polysaccharides at room temperature.[2]

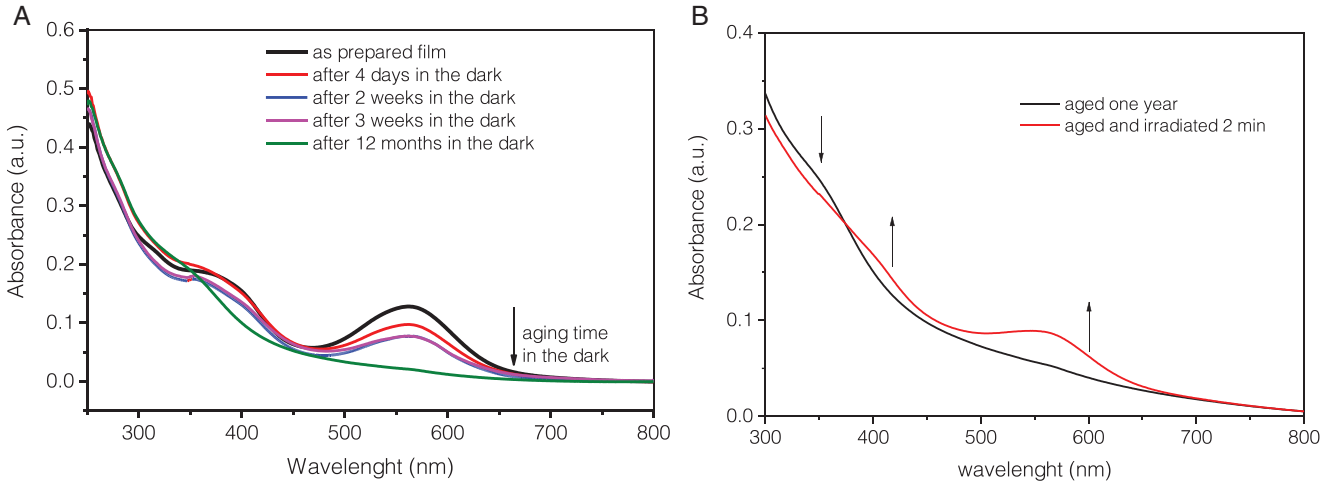

Figure 9. UV–vis spectra of ASP_{100} film on glass obtained by spin coating from HFIP solutions: a) spectral changes occurring upon ageing in the dark the as prepared film; b) comparison between the film aged 1 year in the dark, and the same after further 2 min of UV irradiation.

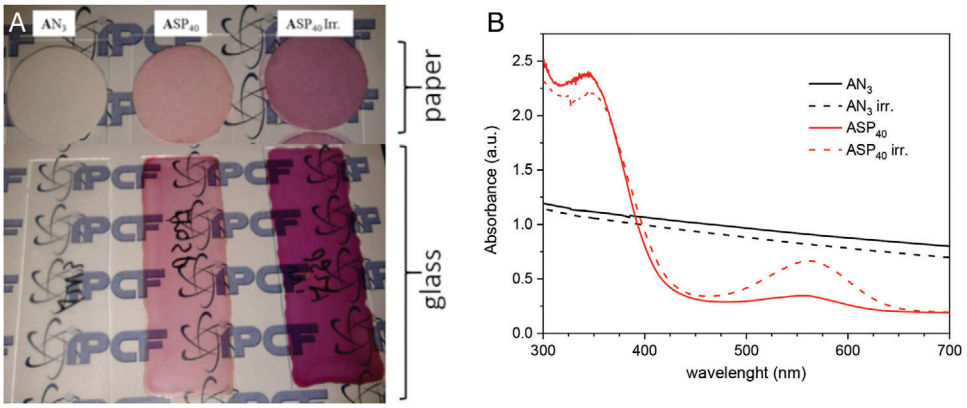

Figure 10. a) Coatings of AN_3 and of ASP_{40} before and after UV irradiation on cast coated glass and dip coated paper; b) UV–vis spectra comparison between AN_3 and ASP_{40} films on glass after (dashed line) and before (solid line) UV irradiation.

Thicker polymer films on glass and coatings on paper were prepared with ASP_{40}, selected because of its better solubility and film forming properties than $ASP_{40}PA_{60}$, and also because the unconverted azides groups may provide additional opportunity for further functionalization or crosslinking.[2] Films on glass were obtained by casting and on paper by dip coating. Glass is inert and transparent in the visible region of the spectrum where MC has its characteristic absorption band. On the other hand, paper is a natural substrate used for many applications and with high affinity for amylose.

Using glass as the substrate, ≈100 μm thick films were prepared by casting from ASP_{40} solution in DMF, one of the three good solvents among those tested for ASP_{40}. A film of AN_3, the precursor of ASP_{40}, was also prepared for comparison. The obtained films were semi-transparent (**Figure 10**a), with some scattering detectable from the nonzero absorption throughout the 300–700 nm range indicating the presence of heterogeneous domains (Figure 10b).

Upon irradiation, the ASP_{40} film turned from pink to intense burgundy red, its UV–vis spectrum showing the typical MC absorption at $\lambda \approx 550$ nm along with a decrease of the SP absorption at $\lambda \approx 350$ nm (Figure 10b). The presence of a weak MC absorption in the as-cast film before irradiation may be ascribed to MC stabilization by solid state interaction with the hydroxyl groups of the polysaccharide; in fact, the casting solvent is unlikely to play any role as the MC absorption of ASP_{40} in DMF solution was negligible, similarly to the case of ASP_{100} in HFIP. Once stored in the dark, the irradiated ASP_{40} film bleached out in about 3 weeks. These results confirm that both the photoactivated SP→MC photoisomerization and the thermal retro-isomerization also occur in the solid state, the rate of the latter process being much slower (several days instead of few minutes) than in solution, but also quite faster for ASP_{40} than for ASP_{100}. Such difference in the retro-isomerization rate could be ascribed to a higher activation energy (by steric hindrance and/or electrostatic interactions among the highly concentrated MC moieties) in ASP_{100} than in ASP_{40}, although some plasticizing contribution from residual DMF, the casting solvent used for ASP_{40} and a much less volatile one than HFIP used to spin coat ASP_{100}, could not be ruled out.

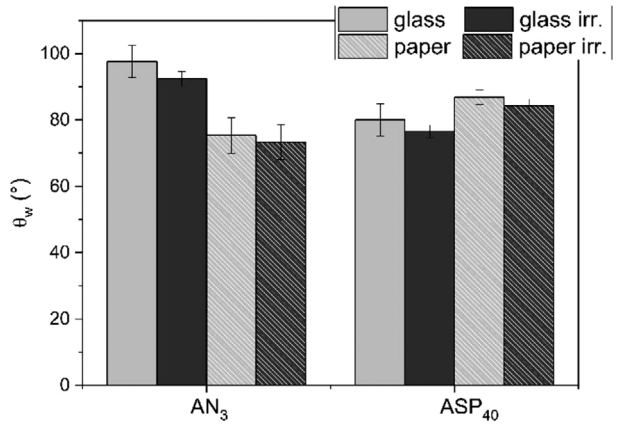

Figure 11. Contact angle value obtained by deposition of a water drop on AN_3 and ASP_{40} coatings on glass and paper before and after exposition under UV light.

Films of ASP_{40} and AN_3 prepared by dip coating on paper showed similar color hue and slightly higher lightness (due to light scattering) as the films on glass, both before and after UV irradiation, indicating that the different substrate and film morphology do not significantly affect the photochromic behavior (Figure 4a).

The static contact angle (**Figure 11**) with water measured on the ASP_{40} film on glass decreased very slightly from 80.0 ± 4.9 to 76.6 ±1.8 deg upon irradiation, as a result of the photoisomerization of the side chain moieties from the neutral and mildly hydrophobic SP to the more hydrophilic zwitterionic MC form. An even higher hydrophobicity was observed for the AN_3 film (contact angle of 97.7 ± 4.4 and 95.5 ± 2.2 deg before and after irradiation, respectively). Thus the mild hydrophobization of the glass substrate upon coating with the modified amylose cannot be specifically ascribed to the SP moieties, but rather to a generic effect of the amylose functionalized with nearly apolar moieties. In all cases the effect of irradiation resulted in negligible decrease of the static water contact angle, irrespective of the occurrence of SP photoisomerization.

4. Conclusions

The effects of photo-isomerization on the solubility of spiropyran-amylose in solvents of different polarity and H-bonding effectiveness allowed to distinguish four distinct behaviors: i) in good solvents (DMF, DMSO) spiropyran is in an equilibrium mixture of closed- and open-ring (zwitterionic or cationic) structure; ii) in poor solvents (water and alcohols) the functionalized polysaccharide is partially or totally in the form of colloidally unstable aggregates but the photo-isomerization of the spiro to MC form is not inhibited; iii) in intermediate solvents, such as THF, the grafted SP moieties of the moderately soluble functionalized polysaccharide are mostly in the apolar spiro-form and can be effectively switched into the MC form by irradiation with UV–vis light, iv) in the very polar HFIP the MC form is preferentially stabilized, resulting in inverse photochromism.

In the solid state the SP→MC photoisomerization and the thermal retro-isomerization processes of the functionalized amylose were not inhibited but only slowed down, as assessed for a thick cast film of ASP_{40}, a thin spin coated film of ASP_{100}, and ASP_{40} coating on paper. While the photoisomerization was always relatively fast, the dynamic change of the thermally activated reversible MC→SP retro-isomerization was quite slower in the solid state than in solution, and was also more clearly affected by the grafting density. The photoisomerization always resulted in significant chromatic changes of the treated substrates. On the other hand, switching the pendant photochromic moieties between the nearly apolar SP and the zwitterionic MC forms in the solid state did not significantly affect the wettability, as shown for the slightly hydrophobic ASP_{40} coating surface. The obtained results suggest that the investigated materials may be used as photochromic coatings for paper, given its good affinity with the SP-modified amylose.

Acknowledgements

This research was partially funded by the University of Ferrara (FAR2021).

Conflict of Interest

The authors declare no conflict of interest.

Data Availability Statement

The data that support the findings of this study are available from the corresponding author upon reasonable request.

Keywords

biobased polymers, click grafting, coatings, paper, photoswitchable coatings

Received: March 29, 2023
Revised: May 29, 2023
Published online: June 17, 2023

[1] V. I. Minkin, *Chem. Rev.* **2004**, *104*, 2751.
[2] M. Bertoldo, S. Nazzi, G. Zampano, F. Ciardelli, *Carbohydr. Polym.* **2011**, *85*, 401.
[3] F. Ciardelli, M. Bertoldo, S. Bronco, A. Pucci, G. Ruggeri, F. Signori, F. Signori, *Polym. Int.* **2013**, *62*, 22.
[4] O. Pieroni, A. Fissi, N. Angelini, F. Lenci, *Acc. Chem. Res.* **2001**, *34*, 9.
[5] A. R. Boyd, P. G. Jessop, J. M. Dust, E. Buncel, *Org. Biomol. Chem.* **2013**, *11*, 6047.
[6] H. Görner, *Chem. Phys. Lett.* **1998**, *282*, 381.
[7] A. Fagan, M. Bartkowski, S. Giordani, *Front. Chem.* **2021**, *9*, 720087.
[8] A. Fissi, O. Pieroni, N. Angelini, F. Lenci, *Macromolecules* **1999**, *32*, 7116.
[9] J. T. C. Wojtyk, A. Wasey, N.-N. Xiao, P. M. Kazmaier, S. Hoz, C. Yu, R. P. Lemieux, E. Buncel, *J. Phys. Chem. A* **2007**, *111*, 2511.
[10] Z. Miskolczy, L. Biczók, *J. Phys. Chem. B* **2011**, *115*, 12577.
[11] M. Hammarson, J. R. Nilsson, S. Li, T. Beke-Somfai, J. Andréasson, *J. Phys. Chem. B* **2013**, *117*, 13561.
[12] J. T. C. Wojtyk, P. M. Kazmaier, E. Buncel, *Chem. Mater.* **2001**, *13*, 2547.

[13] K. H. Fries, J. D. Driskell, G. R. Sheppard, J. Locklin, *Langmuir* **2011**, *27*, 12253.
[14] L. Florea, A. Mckeon, D. Diamond, F. Benito-Lopez, *Langmuir* **2013**, *29*, 2790.
[15] Y. Sheng, J. Leszczynski, A. A. Garcia, R. Rosario, D. Gust, J. Springer, *J. Phys. Chem. B* **2004**, *108*, 16233.
[16] J. B. Flannery, *J. Am. Chem. Soc.* **1968**, *90*, 5660.
[17] H. Li, J. Ding, S. Chen, C. Beyer, S.-X. Liu, H.-A. Wagenknecht, A. Hauser, S. Decurtins, *Chem. - Eur. J.* **2013**, *19*, 6459.
[18] O. M. Mokhtar, Y. Attia, M. Abdelrahman, T. Khattab, *Egypt. J. Chem.* **2022**, *65*, 1175.
[19] J.-I. Edahiro, K. Sumaru, T. Takagi, T. Shinbo, T. Kanamori, *Langmuir* **2006**, *22*, 5224.
[20] R. Klajn, *Chem. Soc. Rev.* **2014**, *43*, 148.
[21] G. Baillet, M. Campredon, R. Guglielmetti, G. Giusti, C. Aubert, *J. Photochem. Photobiol., A* **1994**, *83*, 147.
[22] G. Baillet, G. Giusti, R. Guglielmetti, *J. Photochem. Photobiol., A* **1993**, *70*, 157.
[23] A. Radu, R. Byrne, N. Alhashimy, M. Fusaro, S. Scarmagnani, D. Diamond, *J. Photochem. Photobiol., A* **2009**, *206*, 109.
[24] J. Keyvan Rad, A. R. Mahdavian, *J. Phys. Chem. C* **2016**, *120*, 9985.
[25] A. S. Kozlenko, I. V. Ozhogin, A. D. Pugachev, M. B. Lukyanova, I. M. El-Sewify, B. S. Lukyanov, *Top. Curr. Chem.* **2023**, *381*, 8.
[26] A. A. Ali, R. Kharbash, Y. Kim, *Anal. Chim. Acta* **2020**, *1110*, 199.
[27] G. C. Thaggard, J. Haimerl, K. C. Park, J. Lim, R. A. Fischer, B. K. P. Maldeni Kankanamalage, B. J. Yarbrough, G. R. Wilson, N. B. Shustova, *J. Am. Chem. Soc.* **2022**, *144*, 23249.
[28] A. Bianco, S. Perissinotto, M. Garbugli, G. Lanzani, C. Bertarelli, *Laser Photonics Rev.* **2011**, *5*, 711.
[29] J. T. C. Wojtyk, A. Wasey, P. M. Kazmaier, S. Hoz, E. Buncel, *J. Phys. Chem. A* **2000**, *104*, 9046.
[30] A. Abdollahi, H. Roghani-Mamaqani, B. Razavi, *Prog. Polym. Sci.* **2019**, *98*, 101149.
[31] J. Keyvan Rad, Z. Balzade, A. R. Mahdavian, *J. Photochem. Photobiol., C* **2022**, *51*, 100487.
[32] L. Kortekaas, W. R. Browne, *Chem. Soc. Rev.* **2019**, *48*, 3406.
[33] K. Arai, Y. Shitara, T. Ohyama, *J. Mater. Chem.* **1996**, *6*, 11.
[34] C. Cui, G. Liu, H. Gao, M. Wang, J. Gao, *Polymer* **2022**, *253*, 124995.
[35] A. S. Kritchenkov, Y. A. Skorik, *Russ. Chem. Bull.* **2017**, *66*, 769.
[36] G. Hong, H. Zhang, Y. Lin, Y. Chen, Y. Xu, W. Weng, H. Xia, *Macromolecules* **2013**, *46*, 8649.
[37] D. Barsi, S. Borsacchi, L. Calucci, A. Tarantino, C. Pinzino, M. Bertoldo, *Polymer* **2017**, *120*, 82.
[38] W. Tian, J. Tian, *Langmuir* **2014**, *30*, 3223.
[39] J. Shey, K. M. Holtman, R. Y. Wong, K. S. Gregorski, A. P. Klamczynski, W. J. Orts, G. M. Glenn, S. H. Imam, *Carbohydr. Polym.* **2006**, *65*, 529.
[40] H. Falk, M. Stanek, *Monatsh. Chem.* **1997**, *128*, 777.
[41] Y. Marcus, *The properties of solvents*, Wiley, Chichester, NY **1998**.
[42] A. Imberty, H. Chanzy, S. Pérez, A. Bulèon, V. Tran, *J. Mol. Biol.* **1988**, *201*, 365.
[43] A. Imberty, S. Perez, *Biopolymers* **1988**, *27*, 1205.
[44] P. Joseph, K. Kundu, P. K. Kundu, *ChemistrySelect* **2018**, *3*, 11065.
[45] J. Biteau, F. Chaput, J.-P. Boilot, *J. Phys. Chem.* **1996**, *100*, 9024.
[46] G. Smets, in *Unusual Properties of New Polymers*, Springer, Berlin **2005**, pp. 17–44.

